

Multiple-node model of wind turbine generating system for unbalanced distribution system load flow analysis

Rudy Gianto, Kho Hie Khwee

Department of Electrical Engineering, Faculty of Engineering, Tanjungpura University, Pontianak, Indonesia

Article Info

Article history:

Received Dec 10, 2022

Revised Jun 23, 2023

Accepted Sep 11, 2023

Keywords:

Induction generator

Load flow

Multiple-node model

Unbalanced distribution system

Wind turbine generating system

ABSTRACT

This paper discusses a method to integrate a wind turbine generating system (WTGS) into a three-phase unbalanced distribution system load flow (DSLF) analysis. The proposed method is based on the single-phase multiple-node model. In the present work, the single-phase multiple-node model is extended to a three-phase multiple-node model to facilitate the load flow analysis of a three-phase unbalanced power system network. The multiple-node model (i.e., three-node model) will only modify the load flow analysis by introducing two lines and two load buses to the distribution system network where the WTGS is installed. Thus, a standard three-phase load flow program can be employed to compute the unknown quantities in the DSLF problem formulation. The proposed method is verified by incorporating the model into the load flow analysis of three-phase distribution networks. The investigation uses two representative distribution networks (i.e., 19-bus and 25-bus networks). The results of the study confirm the validity of the proposed method.

This is an open access article under the [CC BY-SA](#) license.



Corresponding Author:

Rudy Gianto

Department of Electrical Engineering, Faculty of Engineering, Tanjungpura University

St. Prof. Dr. H. Hadari Nawawi, Pontianak, 78124, Indonesia

Email: rudy.gianto@ee.untan.ac.id

1. INTRODUCTION

In general, the electric power distribution system is highly unbalanced. The system unbalance is mainly caused by: i) uneven loads on each phase; and/or ii) untransposed distribution lines. Due to the unbalance, the single-phase approach can no longer be used to analyze such a system, and a three-phase method should be used instead [1], [2]. Moreover, the integration of distributed generations with renewable energy sources in the electric power distribution system has also increased recently. It has been acknowledged that primary energy sources for distributed renewable energy generation include: wind power, solar photovoltaic, and hydropower. However, wind-driven electric power generation systems are more established in technology development among the three energy sources and have broader applications [3]–[5]. Since the penetration of wind turbine generating system (WTGS) in electric power distribution systems has been increasing significantly, the assessment of the system's steady-state performance will be more difficult. Generally, the system steady-state performance assessment is carried out based on the results of load flow analysis. The first and probably most critical step in the analysis is to model all system components. Several attractive techniques for integrating WTGS in steady-state load flow analysis have been proposed in [6]–[23].

An exciting method to incorporate the WTGS model into a standard load flow program has been proposed in [6]–[8]. The inclusion of the WTGS adds two buses (nodes), two series elements, one shunt element, and one load on the existing power system network. A mathematical model of WTGS has been

developed in [9]–[11]. This mathematical equation (together with the existing load flow equation) is then solved iteratively. Various steady-state load flow models of fixed-speed WTGS have been proposed in [12], [13]. The models are developed based on the equivalent circuits of the induction generator. These mathematical models are combined with the steady-state models of the system without WTGS and then solved simultaneously. Some methods for integrating variable speed WTGS have been proposed in [14]–[20]. The WTGS models in [14]–[20], are also derived based on the steady-state equivalent circuits of the generator used by the WTGS. Steady-state three-phase models of WTGS have been developed in [21]–[23]. The models in [21]–[23] can be incorporated and applied in the load flow analysis of unbalanced electric power systems.

In the methods proposed in [16]–[20] the power system has been assumed to be balanced, and the single-phase load flow has been used in the analysis. Since, as previously mentioned, the electric power distribution system is generally unbalanced, and the single-phase load flow approach is no longer adequate to analyze such a system. Although the proposed methods in [21]–[23] can be used to integrate the WTGS into an unbalanced system's load flow analysis, a standard three-phase load flow program can not be employed to obtain the solution. The program has to be modified to include the WTGS mathematical model in the calculation.

Therefore, against the above background, the objective of the present paper is to develop the WTGS model that can facilitate the load flow analysis in a three-phase unbalanced power system network without the need to modify the standard load flow program. The present work proposes the extension of the single-phase multiple-node model [6]–[8] to a three-phase multiple-node model. The model is incorporated into the load flow analysis of a three-phase unbalanced distribution network. A standard three-phase load flow program can then be employed to compute the unknown quantities in the distribution system load flow (DSL) problem formulation. The rest of the paper is organized as follows: section 2 addresses the single-phase multiple-node model of WTGS. The extension of the single-phase multiple-node model to the three-phase multiple-node model is given in section 3. Section 4 discusses study cases where validation of the proposed method is presented. Finally, some important conclusions of the paper are pointed out in section 5.

2. MULTIPLE-NODE MODEL OF WTGS

Figures 1 and 2 show induction generator equivalent circuits of WTGS connected to an electric power system at bus k [6]–[10]. It is to be noted that both of the equivalent circuits in Figures 1 and 2 are valid and can be used to represent the WTGS induction generator. In Figure 1, P_m is turbine mechanical power input, S_g is WTGS electric power output, V_S and V_R are stator and rotor voltages, I_S and I_R are stator and rotor currents, and s is induction generator slip. Also, in Figure 2, Z_S and Z_R are stator and rotor circuit impedances, and Y_M is magnetic core circuit admittance. These impedances and admittance are determined based on the induction generator resistances/reactances and have the following forms:

$$Z_S = R_S + jX_S \quad (1)$$

$$Z_R = R_R + jX_R \quad (2)$$

$$Y_M = (R_c + jX_m)/jR_cX_m \quad (3)$$

where R_S/X_S is resistance/reactance of stator circuit, R_R/X_R is resistance/reactance of rotor circuit, and R_c/X_m is resistance/reactance of magnetic core circuit.

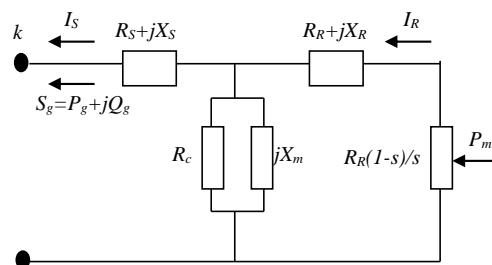


Figure 1. Equivalent circuit of induction generator (per-phase)

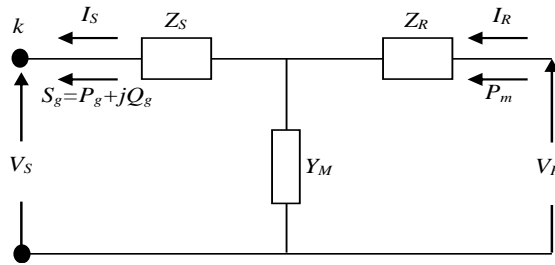


Figure 2. Equivalent circuit of induction generator in terms of impedances (per-phase)

In Figure 1, the turbine mechanical power input is represented by the active power consumed by the variable resistance ($R_R(1-s)/s$). By looking at Figure 1, this mechanical power can be expressed as (4):

$$P_m = -R_R \frac{1-s}{s} I_R I_R^* \quad (4)$$

Based on (4), an equivalent constant power source can therefore be used to represent the variable resistance, as shown in Figure 2. Thus, (4) can be eliminated from the load flow equations, and slip s can also be excluded from the load flow calculations. It should be noted that the value of turbine mechanical power is usually available or known since the turbine manufacturer generally provides the turbine mechanical power curve. Based on the power curve, the turbine mechanical powers, for any wind speed values, can then be determined.

Based on the above discussion, the WTGS induction generator model can be converted into a three-node model in the load flow analysis [6]–[8]. Figure 3 shows the three-node model of the WTGS connected to bus k of an electric power system. In Figure 3, it has been assumed that the power system has n buses and m branches. The three-node model application will modify the load flow analysis by adding two lines and two load buses to the original system network where the WTGS is installed. Thus, a standard load flow program can be employed to compute the unknown quantities in the DLSF problem formulation. Modification to the source code program does not need to be carried out. What needs to be done is to change only the program data input due to the additional lines and buses.

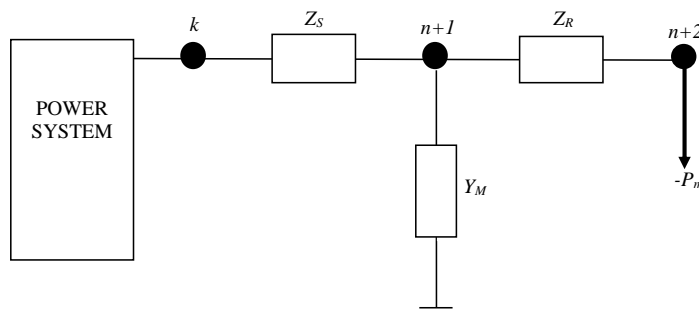


Figure 3. Multiple-node model of WTGS

Detail of the branch and bus data added to the original system network are shown in Tables 1 and 2. The parameters in Tables 1 and 2 are the additional data input to the load flow program due to the WTGS installation at bus k . It can be seen from Table 1 that the turbine mechanical power is treated as a load with negative power ($-P_m$). The value of P_m , as mentioned earlier, can be determined based on the power curve provided by the turbine manufacturer. It should also be noted that Z_S , Z_R , and Y_M are calculated using (1).

Table 1. Addition of bus data

Bus	Power generation	Power demand	Shunt admittance
$n+1$	0	0	Y_M
$n+2$	0	$-P_m$	0

Table 2. Addition of branch data

Line	Bus p to q	Series impedance (Z)	Half line shunt admittance ($Y_{sh}/2$)
$m+1$	k to $n+1$	Z_S	0
$m+2$	$n+1$ to $n+2$	Z_R	0

3. MULTIPLE-NODE MODEL OF WTGS FOR THREE-PHASE DSLF ANALYSIS

Figure 4 shows the application of the three-node model in a three-phase electrical power system network. Figure 4 is obtained based on Figure 3, where the impedances of the induction generator (i.e., Z_S , Z_R , and Y_M) have been represented by 3×3 matrices to facilitate the analysis in a three-phase network. Detail of the branch and bus parameters added to the power system due to WTGS installation are presented in Tables 3 and 4. In Tables 3 and 4, the elements of 3×3 series impedance and shunt admittance matrices are calculated as (5)-(7):

$$Z_S^{uv} = R_S^{uv} + jX_S^{uv} \quad (5)$$

$$Z_R^{uv} = R_R^{uv} + jX_R^{uv} \quad (6)$$

$$Y_M^{uv} = (R_c^{uv} + jX_m^{uv})/jR_c^{uv} X_m^{uv} \quad (7)$$

where $u=a, b, c$ and $v=a, b, c$. Also, the elements of turbine mechanical power vector can be determined using:

$$P_m^a = P_m^b = P_m^c = \frac{P_m}{3} \quad (8)$$

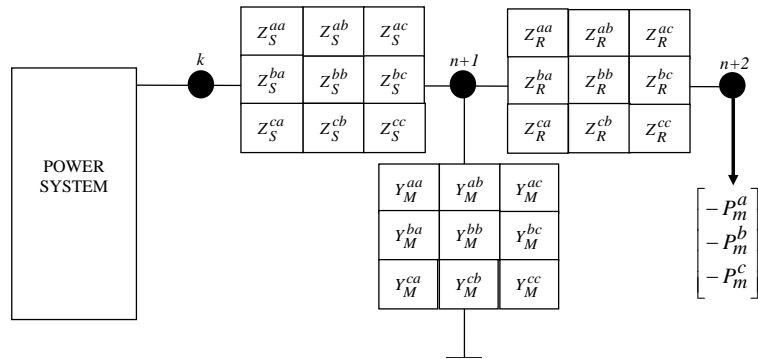


Figure 4. Multiple-node model for three-phase power flow

Table 3. Addition of bus data for three-phase system

Bus	Power generation	Power demand	Shunt admittance
$n+1$	$\begin{bmatrix} 0 \\ 0 \\ 0 \end{bmatrix}$	$\begin{bmatrix} 0 \\ 0 \\ 0 \end{bmatrix}$	$\begin{bmatrix} Y_M^{aa} & Y_M^{ab} & Y_M^{ac} \\ Y_M^{ba} & Y_M^{bb} & Y_M^{bc} \\ Y_M^{ca} & Y_M^{cb} & Y_M^{cc} \end{bmatrix}$
$n+2$	$\begin{bmatrix} 0 \\ 0 \\ 0 \end{bmatrix}$	$\begin{bmatrix} -P_m^a \\ -P_m^b \\ -P_m^c \end{bmatrix}$	$\begin{bmatrix} 0 & 0 & 0 \\ 0 & 0 & 0 \\ 0 & 0 & 0 \end{bmatrix}$

Table 4. Addition of branch data for three-phase system

Line	Bus p to q	Series impedance (Z)	Half line shunt admittance ($Y_{sh}/2$)
$m+1$	k to $n+1$	$\begin{bmatrix} Z_S^{aa} & Z_S^{ab} & Z_S^{ac} \\ Z_S^{ba} & Z_S^{bb} & Z_S^{bc} \\ Z_S^{ca} & Z_S^{cb} & Z_S^{cc} \end{bmatrix}$	$\begin{bmatrix} 0 & 0 & 0 \\ 0 & 0 & 0 \\ 0 & 0 & 0 \end{bmatrix}$
$m+2$	$n+1$ to $n+2$	$\begin{bmatrix} Z_R^{aa} & Z_R^{ab} & Z_R^{ac} \\ Z_R^{ba} & Z_R^{bb} & Z_R^{bc} \\ Z_R^{ca} & Z_R^{cb} & Z_R^{cc} \end{bmatrix}$	$\begin{bmatrix} 0 & 0 & 0 \\ 0 & 0 & 0 \\ 0 & 0 & 0 \end{bmatrix}$

4. CASE STUDY

4.1. Case study 1

The first case study is based on 19-bus network. A single-line diagram of the network is shown in Figure 5. It is an unbalanced network with a system voltage of 11 kV [23]. The system has a total three-phase load of 515.94 kW and 177.27 kVAR (phase-a: 176.33 kW and 61.23 kVAR; phase-b: 166.34 kW and

56.34 kVAR; phase-c: 173.27 kW and 59.70 kVAR). Detail of the system data including the WTGS data can be found in [23]. Results of the load flow analysis for the system are shown in Tables 5-7. In Tables 5-7, the values in pu are on a 1 MVA base. It is to be noted that the results in Tables 5-7 are in excellent agreement with the results in [23], which confirm the correctness of the proposed method.

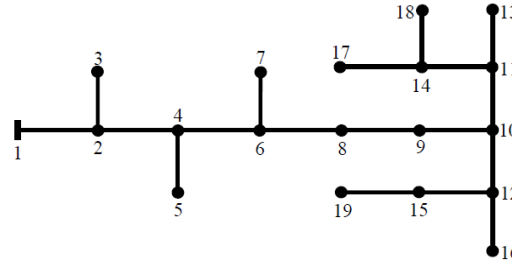


Figure 5. 19-bus network

Table 5. 19-bus network WTGS voltages (in pu)

P_m (pu)	Phase-a	Phase-b	Phase-c
0.03	$0.91787\angle 1.09^\circ$	$0.91590\angle -118.91^\circ$	$0.91671\angle 121.05^\circ$
0.06	$0.92543\angle 1.29^\circ$	$0.92352\angle -118.71^\circ$	$0.92431\angle 121.25^\circ$
0.09	$0.93286\angle 1.49^\circ$	$0.93100\angle -118.51^\circ$	$0.93176\angle 121.45^\circ$
0.12	$0.94015\angle 1.68^\circ$	$0.93835\angle -118.32^\circ$	$0.93908\angle 121.64^\circ$
0.15	$0.94732\angle 1.87^\circ$	$0.94556\angle -118.13^\circ$	$0.94627\angle 121.84^\circ$
0.18	$0.95437\angle 2.06^\circ$	$0.95265\angle -117.94^\circ$	$0.95335\angle 122.03^\circ$
0.21	$0.96131\angle 2.25^\circ$	$0.95963\angle -117.75^\circ$	$0.96030\angle 122.21^\circ$
0.24	$0.96813\angle 2.43^\circ$	$0.96650\angle -117.57^\circ$	$0.96715\angle 122.40^\circ$
0.27	$0.97485\angle 2.62^\circ$	$0.97326\angle -117.38^\circ$	$0.97389\angle 122.58^\circ$
0.30	$0.98147\angle 2.80^\circ$	$0.97991\angle -117.20^\circ$	$0.98053\angle 122.76^\circ$

Table 6. 19-bus network WTGS power outputs (in pu)

P_m (pu)	Phase-a	Phase-b	Phase-c
0.03	$0.00831-j0.03369$	$0.00832-j0.03355$	$0.00832-j0.03360$
0.06	$0.01828-j0.03425$	$0.01829-j0.03411$	$0.01829-j0.03417$
0.09	$0.02825-j0.03482$	$0.02826-j0.03468$	$0.02826-j0.03474$
0.12	$0.03822-j0.03538$	$0.03823-j0.03525$	$0.03823-j0.03530$
0.15	$0.04819-j0.03594$	$0.04820-j0.03581$	$0.04820-j0.03586$
0.18	$0.05816-j0.03650$	$0.05817-j0.03637$	$0.05816-j0.03643$
0.21	$0.06813-j0.03706$	$0.06814-j0.03694$	$0.06813-j0.03699$
0.24	$0.07810-j0.03762$	$0.07810-j0.03750$	$0.07810-j0.03755$
0.27	$0.08806-j0.03818$	$0.08807-j0.03806$	$0.08807-j0.03810$
0.30	$0.09803-j0.03874$	$0.09804-j0.03861$	$0.09803-j0.03866$

Table 7. 19-bus network substation power outputs (in pu)

P_m (pu)	Phase-a	Phase-b	Phase-c
0.03	$0.17969+j0.09995$	$0.16982+j0.09493$	$0.17684+j0.09843$
0.06	$0.16840+j0.09995$	$0.15849+j0.09492$	$0.16552+j0.09841$
0.09	$0.15730+j0.10003$	$0.14735+j0.09499$	$0.15440+j0.09848$
0.12	$0.14638+j0.10019$	$0.13640+j0.09514$	$0.14346+j0.09862$
0.15	$0.13564+j0.10042$	$0.12562+j0.09536$	$0.13270+j0.09884$
0.18	$0.12506+j0.10072$	$0.11502+j0.09566$	$0.12210+j0.09912$
0.21	$0.11465+j0.10108$	$0.10458+j0.09602$	$0.11167+j0.09948$
0.24	$0.10439+j0.10152$	$0.09429+j0.09645$	$0.10140+j0.09990$
0.27	$0.09428+j0.10201$	$0.08415+j0.09694$	$0.09127+j0.10039$
0.30	$0.08431+j0.10257$	$0.07416+j0.09749$	$0.08128+j0.10093$

4.2. Case study 2

The second case study is based on 25-bus network. A single-line diagram of the network is given in Figure 6. It is also an unbalanced network with a system voltage of 4.16 kV [24], [25]. The system has a total three-phase load of 11,145 kW and 2,884 kVAR (phase-a: 1,298.3 kW and 957 kVAR; phase-b: 3,919.9 kW and 967 kVAR; phase-c: 1,303.3 kW and 960 kVAR). All of the system data can be found in [24], [25]. A WTGS with a power rating of 3 MW is assumed to be connected to bus 25. Data of the WTGS (i.e., induction generator impedances) are shown in Table 8.

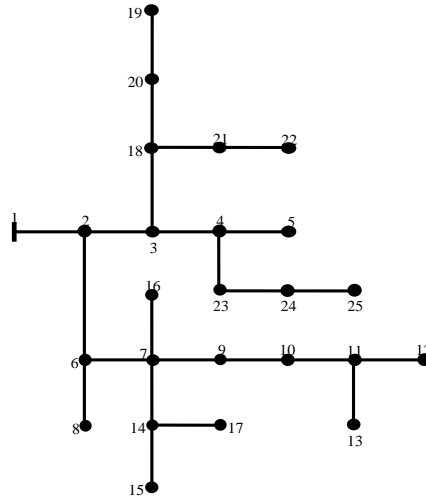


Figure 6. 25-bus network

Tables 9-12 show the load flow analysis results for the unbalanced 25-bus distribution system. In Tables 9-12, the values in pu are also on a 1 MVA base. Since the system is unbalanced, the electrical quantities of the three phases are not identical. The results in Tables 9-12 are also given in the form of graphics as shown in Figures 7-9. Figure 7 indicates that the system voltage profile improves as the amount of turbine mechanical power is raised. This improvement is due to increased WTGS or wind power plant (WPP) output. This WTGS output increment implies that the power injection at the WTGS bus also increases, reducing the line losses and improving the system voltage profile.

Table 8. WTGS data

Parameter	Resistance/reactance value (Ohm)
Stator circuit	Self: $R_S^{aa} = R_S^{bb} = R_S^{cc} = 0.057685$; $X_S^{aa} = X_S^{bb} = X_S^{cc} = 0.288427$
	Mutual: $R_S^{ab} = R_S^{ac} = R_S^{bc} = 0$; $X_S^{ab} = X_S^{ac} = X_S^{bc} = 0$
Rotor circuit	Self: $R_R^{aa} = R_R^{bb} = R_R^{cc} = 0.057685$; $X_R^{aa} = X_R^{bb} = X_R^{cc} = 0.288427$
	Mutual: $R_R^{ab} = R_R^{ac} = R_R^{bc} = 0$; $X_R^{ab} = X_R^{ac} = X_R^{bc} = 0$
Core circuit	Self: $R_C^{aa} = R_C^{bb} = R_C^{cc} = 576.85$; $X_m^{aa} = X_m^{bb} = X_m^{cc} = 28.84$
	Mutual: $(R_m^{ab})^{-1} = (R_m^{ac})^{-1} = (R_m^{bc})^{-1} = 0$; $(X_m^{ab})^{-1} = (X_m^{ac})^{-1} = (X_m^{bc})^{-1} = 0$

Table 9. 25-bus network WTGS voltages (in pu)

P_m (pu)	Phase-a	Phase-b	Phase-c
0.3	$0.92143 \angle 0.26^\circ$	$0.92619 \angle -119.54^\circ$	$0.93473 \angle 119.90^\circ$
0.6	$0.92937 \angle 0.74^\circ$	$0.93421 \angle -119.10^\circ$	$0.94136 \angle 120.35^\circ$
0.9	$0.93698 \angle 1.22^\circ$	$0.94185 \angle -118.65^\circ$	$0.94767 \angle 120.80^\circ$
1.2	$0.94402 \angle 1.70^\circ$	$0.94914 \angle -118.21^\circ$	$0.95365 \angle 121.25^\circ$
1.5	$0.95078 \angle 2.19^\circ$	$0.95610 \angle -117.76^\circ$	$0.96033 \angle 121.70^\circ$
1.8	$0.95720 \angle 2.67^\circ$	$0.96275 \angle -117.31^\circ$	$0.96673 \angle 122.16^\circ$
2.1	$0.96329 \angle 3.16^\circ$	$0.96910 \angle -116.86^\circ$	$0.97285 \angle 122.61^\circ$
2.4	$0.96908 \angle 3.65^\circ$	$0.97517 \angle -116.41^\circ$	$0.97970 \angle 123.07^\circ$
2.7	$0.97456 \angle 4.14^\circ$	$0.98097 \angle -115.96^\circ$	$0.98530 \angle 123.53^\circ$
3.0	$0.97976 \angle 4.63^\circ$	$0.98651 \angle -115.50^\circ$	$0.99064 \angle 124.00^\circ$

Table 10. 25-bus network WTGS power outputs (in pu)

P_m (pu)	Phase-a	Phase-b	Phase-c
0.3	0.09110-j0.16958	0.09102-j0.17131	0.09086-j0.17444
0.6	0.19025-j0.17626	0.19017-j0.17800	0.19005-j0.18058
0.9	0.28897-j0.18495	0.28890-j0.18669	0.28881-j0.18874
1.2	0.38729-j0.19556	0.38723-j0.19729	0.38717-j0.19882
1.5	0.48521-j0.20800	0.48517-j0.20970	0.48514-j0.212075
1.8	0.58276-j0.22219	0.58274-j0.22386	0.58274-j0.22446
2.1	0.67996-j0.23810	0.67997-j0.23970	0.67997-j0.23991
2.4	0.77680-j0.25565	0.77684-j0.25717	0.77684-j0.25755
2.7	0.87330-j0.27482	0.87339-j0.27622	0.87336-j0.27685
3.0	0.96946-j0.29557	0.96961-j0.29682	0.96955-j0.29728

Table 11. 25-bus network substation power outputs (in pu)

P_m (pu)	Phase-a	Phase-b	Phase-c
0.3	1.28992+j1.22132	1.31299+j1.22448	1.27542+j1.22218
0.6	1.18524+j1.22279	1.20819+j1.22568	1.17266+j1.22301
0.9	1.08312+j1.22438	1.10594+j1.22878	1.07202+j1.22575
1.2	0.98340+j1.23188	1.00609+j1.23658	0.97341+j1.23323
1.5	0.88496+j1.24309	0.90752+j1.24789	0.87476+j1.24429
1.8	0.79071+j1.25786	0.81313+j1.26256	0.78198+j1.25880
2.1	0.69755+j1.27605	0.71983+j1.28044	0.68901+j1.27666
2.4	0.60641+j1.29756	0.62855+j1.30144	0.59781+j1.29779
2.7	0.51723+j1.32228	0.53922+j1.32544	0.50834+j1.32210
3.0	0.42996+j1.35016	0.45180+j1.35239	0.42056+j1.34954

Table 12. 25-bus network WTGS/substation total outputs and line losses (in pu)

P_m (pu)	WPP	Substation	line losses
0.3	0.27298-j0.51533	3.87833+j3.66798	0.23141+j0.26865
0.6	0.57047-j0.53484	3.56609+j3.67148	0.21666+j0.25264
0.9	0.86668-j0.56038	3.26108+j3.67891	0.20786+j0.23453
1.2	1.16169-j0.59167	2.96290+j3.70169	0.20469+j0.22602
1.5	1.45552-j0.62845	2.66724+j3.73528	0.20286+j0.22283
1.8	1.74824-j0.67051	2.38582+j3.77922	0.21416+j0.22471
2.1	2.03990-j0.71771	2.10639+j3.83316	0.22639+j0.23145
2.4	2.33048-j0.77037	1.83277+j3.89678	0.24335+j0.24241
2.7	2.62005-j0.82789	1.56479+j3.96983	0.26494+j0.25794
3.0	2.90862-j0.88967	1.30232+j4.05208	0.29104+j0.27841

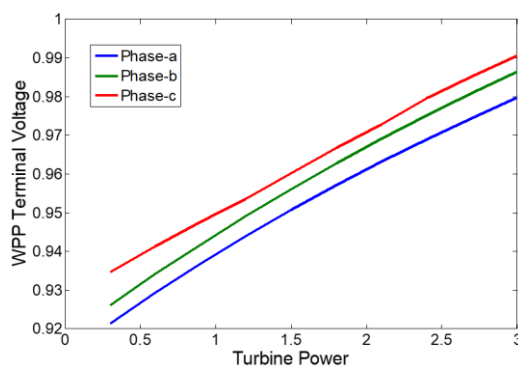


Figure 7. Variation of WPP voltages

Figures 8(a) and (b) show the variations of WTGS power outputs against turbine mechanical power inputs. Figure 8(a) shows that with the increase in turbine power, the WTGS active power output also linearly increases. However, the WTGS active power is slightly smaller than turbine power due to the power loss in the induction generator. Figure 8(b) shows that with the increase in turbine power, the rise in WTGS reactive power demand is not linear but more rapid or almost exponential. This higher demand for reactive power is because more reactive power is needed to magnetize the induction generator as the WTGS active power increases.

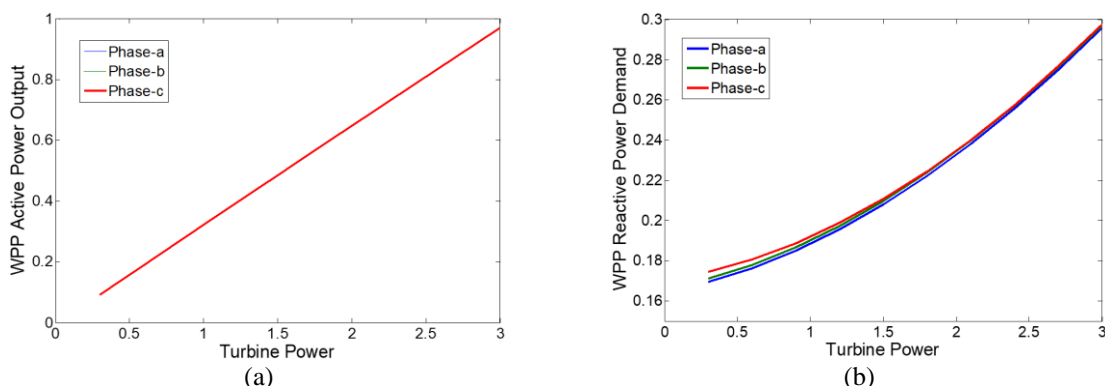


Figure 8. Variation of WPP outputs; (a) active power and (b) reactive power

Since the WTGS can fulfill some load demands, the power supply (active power) from the distribution substation can significantly be reduced as the WTGS active power output increases as shown in Figure 9(a). On the other hand, the substation reactive power will increase as the turbine mechanical power (i.e., the WTGS active power output) is raised as shown in Figure 9(b). This increase in reactive power due to more reactive power is needed for the induction generator magnetization as the WTGS active power increases.

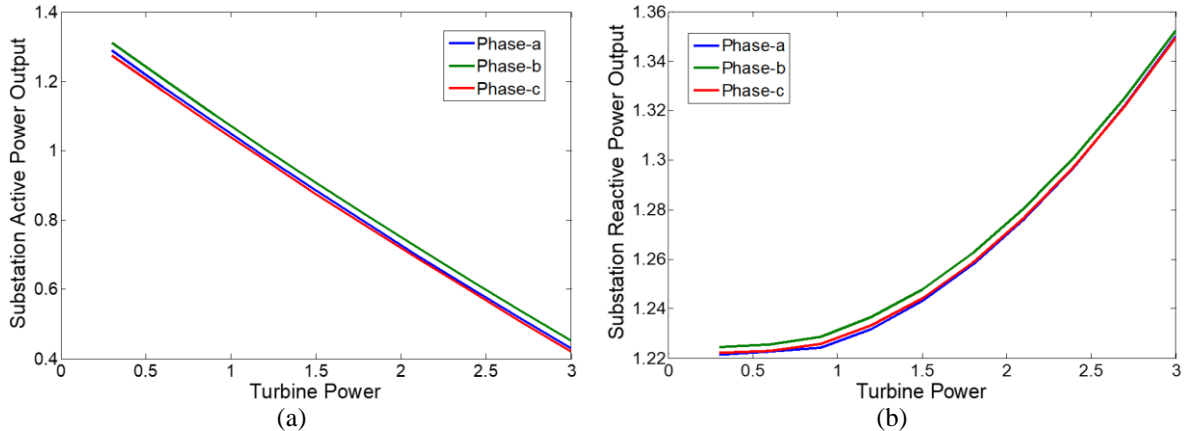


Figure 9. Variation of substation outputs (a) active power and (b) reactive power

5. CONCLUSION

A method to integrate WTGS into a three-phase unbalanced DSLF analysis has been proposed in this paper. The present work extends the single-phase multiple-node model to a three-phase multiple-node model. The model is then incorporated into the load flow analysis of a three-phase power distribution network. Application of the multiple-node model will only modify the load flow analysis by adding two lines and two load buses to the distribution system network where the WTGS is installed. Thus, a standard load flow program can be employed to compute the unknown quantities in the DSLF problem formulation. Modification to the source code program does not need to be carried out. What needs to be done is to change only the program data input due to the additional lines and buses. This paper has used two representative three-phase distribution networks (i.e., 19-bus and 25-bus networks) to confirm and validate the proposed method.

ACKNOWLEDGEMENTS

The authors would like to express special appreciation to the Ministry of Education, Culture, Research, and Technology (Kemendikbudristek Republik Indonesia) for providing the grant to conduct the research reported in this paper.

REFERENCES

- [1] U. Ghatak and V. Mukherjee, "A fast and efficient load flow technique for unbalanced distribution system," *International Journal of Electrical Power and Energy Systems*, vol. 84, pp. 99–110, Jan. 2017, doi: 10.1016/j.ijepes.2016.05.002.
- [2] B. Sereeter, K. Vuik, and C. Witteveen, "Newton power flow methods for unbalanced three-phase distribution networks," *Energies*, vol. 10, no. 10, Oct. 2017, doi: 10.3390/en10101658.
- [3] K. Moloi, Y. Hamam, and J. A. Jordaan, "Towards optimal planning of renewable energy mix power integration with distribution system-A review," *International Review of Electrical Engineering*, vol. 16, no. 1, pp. 17–40, Feb. 2021, doi: 10.15866/iree.v16i1.19278.
- [4] E. R. Mmary and B. Marungsri, "Integration of renewable energy distributed generation and battery energy storage in radial power distribution system," *International Energy Journal*, vol. 19, no. 1, pp. 27–36, 2019.
- [5] R. Verma and V. Sarkar, "Active distribution network load flow analysis through non-repetitive FBS iterations with integrated DG and transformer modelling," *IET Generation, Transmission and Distribution*, vol. 13, no. 4, pp. 478–484, Jan. 2019, doi: 10.1049/iet-gtd.2018.5478.
- [6] M. H. Haque, "Evaluation of power flow solutions with fixed speed wind turbine generating systems," *Energy Conversion and Management*, vol. 79, pp. 511–518, Mar. 2014, doi: 10.1016/j.enconman.2013.12.049.
- [7] J. Wang, C. Huang, and A. F. Zobaa, "Multiple-node models of asynchronous wind turbines in wind farm for load flow analysis," *Electric Power Components and Systems*, vol. 44, no. 2, pp. 135–141, Dec. 2016, doi: 10.1080/15325008.2015.1102180.
- [8] M. H. Haque, "Incorporation of fixed speed wind turbine generators in load flow analysis of distribution systems," *International Journal of Renewable Energy Technology*, vol. 6, no. 4, p. 317, 2015, doi: 10.1504/ijret.2015.072099.
- [9] A. Feijoo and D. Villanueva, "A PQ model for asynchronous machines based on rotor voltage calculation," *IEEE Transactions on*

- Energy Conversion*, vol. 31, no. 2, pp. 813–814, Jun. 2016, doi: 10.1109/TEC.2016.2529502.
- [10] A. Feijoo and D. Villanueva, “Correction to ‘A PQ model for asynchronous machines based on rotor voltage calculation,’” *IEEE Transactions on Energy Conversion*, vol. 31, no. 3, pp. 1228–1228, 2016.
- [11] A. Feijoo, J. L. Pazos, and D. Villanueva, “Conventional asynchronous wind turbine models mathematical expressions for the load flow analysis,” *International Journal of Energy Engineering*, vol. 3, no. 6, pp. 269–278, Dec. 2013, doi: 10.5963/ijee0306008.
- [12] R. Gianto, K. H. Khwee, H. Priyatman, and M. Rajagukguk, “Two-port network model of fixed-speed wind turbine generator for distribution system load flow analysis,” *Telkommika (Telecommunication Computing Electronics and Control)*, vol. 17, no. 3, pp. 1569–1576, Jun. 2019, doi: 10.12928/TELKOMNIKA.V17I3.11866.
- [13] R. Gianto and K. H. Khwee, “A new t-circuit model of wind turbine generator for power system steady state studies,” *Bulletin of Electrical Engineering and Informatics*, vol. 10, no. 2, pp. 550–558, Apr. 2021, doi: 10.11591/eei.v10i2.2306.
- [14] S. Li, “Power flow modeling to doubly-fed induction generators (DFIGs) under power regulation,” *IEEE Transactions on Power Systems*, vol. 28, no. 3, pp. 3292–3301, Aug. 2013, doi: 10.1109/TPWRS.2013.2251914.
- [15] C. M. Nwosu, S. E. Oti, and C. U. Ogbuka, “Transient and steady state performance analysis of power flow control in a DFIG variable speed wind turbine,” *Journal of Electrical Engineering*, vol. 68, no. 1, pp. 31–38, Jan. 2017, doi: 10.1515/jee-2017-0004.
- [16] V. S. S. Kumar and D. Thukaram, “Accurate modeling of doubly fed induction generator based wind farms in load flow analysis,” *Electric Power Systems Research*, vol. 155, pp. 363–371, Feb. 2018, doi: 10.1016/j.epsr.2017.09.011.
- [17] C. V. S. Anirudh and V. S. S. Kumar, “Enhanced modelling of doubly fed induction generator in load flow analysis of distribution systems,” *IET Renewable Power Generation*, vol. 15, no. 5, pp. 980–989, Jan. 2021, doi: 10.1049/rpg2.12077.
- [18] R. Gianto, “Steady-state model of DFIG-based wind power plant for load flow analysis,” *IET Renewable Power Generation*, vol. 15, no. 8, pp. 1724–1735, Mar. 2021, doi: 10.1049/rpg2.12141.
- [19] R. Gianto, Purwoharjono, F. Imansyah, R. Kurnianto, and Danial, “Steady-state load flow model of DFIG wind turbine based on generator power loss calculation,” *Energies*, vol. 16, no. 9, Apr. 2023, doi: 10.3390/en16093640.
- [20] M. Benchagra, M. Hilal, Y. Errami, M. Quassaid, and M. Maaroufi, “Modeling and control of SCIG based variable-speed with power factor control,” *International Review on Modelling and Simulations (IREMOS)*, vol. 4, no. 3, 2011.
- [21] A. Dadhania, B. Venkatesh, A. B. Nassif, and V. K. Sood, “Modeling of doubly fed induction generators for distribution system power flow analysis,” *International Journal of Electrical Power and Energy Systems*, vol. 53, no. 1, pp. 576–583, Dec. 2013, doi: 10.1016/j.ijepes.2013.05.025.
- [22] A. Koksoy, O. Ozturk, M. E. Balci, and M. H. Hocaoglu, “A new wind turbine generating system model for balanced and unbalanced distribution systems load flow analysis,” *Applied Sciences (Switzerland)*, vol. 8, no. 4, Mar. 2018, doi: 10.3390/app8040502.
- [23] R. Gianto and Purwoharjono, “Two-port network model of wind turbine generator for three-phase unbalanced distribution system load flow analysis,” *Bulletin of Electrical Engineering and Informatics*, vol. 11, no. 1, pp. 9–19, Feb. 2022, doi: 10.11591/eei.v11i1.3074.
- [24] U. R. Puthireddy, S. Sivanagaraju, and S. Prabandhamkam, “Power flow analysis of three phase unbalanced distribution system,” *International Journal of Advances in Engineering and Technology*, vol. 3, no. 1, pp. 514–524, 2012.
- [25] V. Ganesh, S. Sivanagaraju, and T. Ramana, “Feeder reconfiguration for loss reduction in unbalanced distribution system using genetic algorithm,” *International Journal of Computer and Information Engineering*, vol. 3, no. 4, pp. 1050–1058, 2009.

BIOGRAPHIES OF AUTHORS



Rudy Gianto received B.E, M.E, and Ph.D. degrees from Tanjungpura University in 1991, Bandung Institute of Technology in 1995, and The University of Western Australia in 2009 respectively. Currently, he is a Professor at Tanjungpura University, Indonesia. His research interests include power system analysis, simulation of power system dynamics, and distributed generation. He has published many research papers in international journals and conferences. He can be contacted at email: rudy.gianto@ee.untan.ac.id.



Kho Hie Khwee was born in Pontianak, Indonesia. He received B.E, and M.E degrees from Tanjungpura University in 1991, and Bandung Institute of Technology in 1995, respectively. Currently, he is an Associate Professor at Tanjungpura University, Indonesia. His research interests include analysis of power system, electrical machines, and renewable energy generation. He has published many research papers in international journals and conferences. He can be contacted at email: Andreankhow@yahoo.co.id.